# Polarization Bistability and Resultant Spin Rings in Semiconductor Microcavities

D. Sarkar,[1] S. S. Gavrilov,[2] M. Sich,[1] J. H. Quilter,[1] R. A. Bradley,[1] N. A. Gippius,[3] K. Guda,[1] V. D. Kulakovskii,[2] M. S. Skolnick,[1] and D. N. Krizhanovskii[1,*]

[1]*Department of Physics and Astronomy, University of Sheffield, Sheffield S3 7RH, United Kingdom*
[2]*Institute of Solid State Physics, RAS, Chernogolovka 142432, Russia*
[3]*LASMEA, Universit Blaise Pascal, UMR 6602 CNRS, 63177 Aubière, France and A.M. Prokhorov General Physics Institute, RAS, Moscow 119991, Russia*

(Received 16 July 2010; revised manuscript received 7 October 2010; published 15 November 2010)

The transmission of a pump laser resonant with the lower polariton branch of a semiconductor microcavity is shown to be highly dependent on the degree of circular polarization of the pump. Spin dependent anisotropy of polariton-polariton interactions allows the internal polarization to be controlled by varying the pump power. The formation of spatial patterns, spin rings with a high degree of circular polarization, arising as a result of polarization bistability, is observed. A phenomenological model based on effective semiclassical equations of motion provides a good description of the experimental results. Inclusion of interactions with the incoherent exciton reservoir, which provides spin-independent blueshifts of the polariton modes, is found to be essential.

DOI: 10.1103/PhysRevLett.105.216402 PACS numbers: 71.36.+c, 42.55.Sa, 42.65.Pc

Nonlinear interactions in optical systems result in a variety of important phenomena such as frequency conversion, parametric oscillation, bistability, pattern formation, and self-organization. In this context hybrid light-matter particles, polaritons, which form due to strong exciton-photon coupling in semiconductor microcavities (MCs), attract much attention [1]. Strong nonlinear interactions due to the excitonic component of polaritons lead to stimulated polariton-polariton scattering and optical parametric oscillation [2,3], bistability [4,5], and superfluidity [6,7]. Bose-Einstein condensation of polariton quasiparticles has also been reported [8]. Compared to weakly coupled MC systems, polariton nonlinear interactions are several orders of magnitude stronger [1].

A distinguishing feature of polariton systems arises from their spin properties. Polaritons with parallel spins repel, polaritons with opposite spins attract. Such interactions provide blueshifts and redshifts, respectively, of the energies of coherent polariton modes. This asymmetry results in polarization bistability and multistability predicted recently [9]. Polariton polarization bistability has also been predicted to lead to the formation of spatial spin rings of high degree of circular polarization (DCP) [10]. These nonlinear spin properties and spatial patterns may lead to novel optical spin-based devices such as fast optical modulators, spin switches [10,11], and polariton logic elements (polariton neurons) [12] operating at high picosecond speeds and very low pump powers. Polarization multistability has been studied for a vapor of atoms in a cavity [13,14]. It has been also investigated in a number of solid state nonlinear systems including anisotropic crystals, magnetic cavities, and VCSELs (see Ref. [9], and references therein). However, in the latter structures pump powers a few orders of magnitude stronger then in the polariton system are required to observe nonlinearities, favoring microcavity polaritons for the development of nonlinear optical devices.

In the present work we investigate bistability of spin-up and spin-down polariton fields as a function of the intensity and polarization of an external pump beam. As a result of spin dependent polariton-polariton interactions [9] we are able to switch abruptly the internal polariton DCP by 40%–50% by tuning the pump power. We demonstrate the formation of spatial ring patterns of high DCP, a result of the bistable thresholdlike behavior of the DCP for spatially nonuniform excitation [10]. The pump power behavior and the similar bistability thresholds for spin-up and spin-down coherent polariton components for unequal spin polarized internal fields, indicate the influence of the incoherent exciton reservoir in leading to blueshifts towards resonance of the polarized polariton modes. The experimental results are explained by effective semiclassical equations of motion, taking into account coupling to the reservoir.

We study the transmission of a single-mode cw Ti: sapphire laser at normal incidence ($k = 0$) [Fig. 1(e), inset] in a GaAs-based MC described in Ref. [15] at 5 K. The detuning between exciton and photon modes is close to zero. The energy of the laser is tuned $\sim$0.7 meV above the bottom of the lower polariton (LP) branch (854.8 nm) and $\sim$2 meV below the exciton level [4,5].

A well-known property of the interacting polariton system is bistability of transmitted intensity (or internal polariton field), which has a characteristic *S*-shape dependence versus pump power [4,5]. It is observed at positive detuning between the pump energy and the LP mode. At low pump power the transmission is very low, since the laser energy is out of resonance with the LP mode. With

 

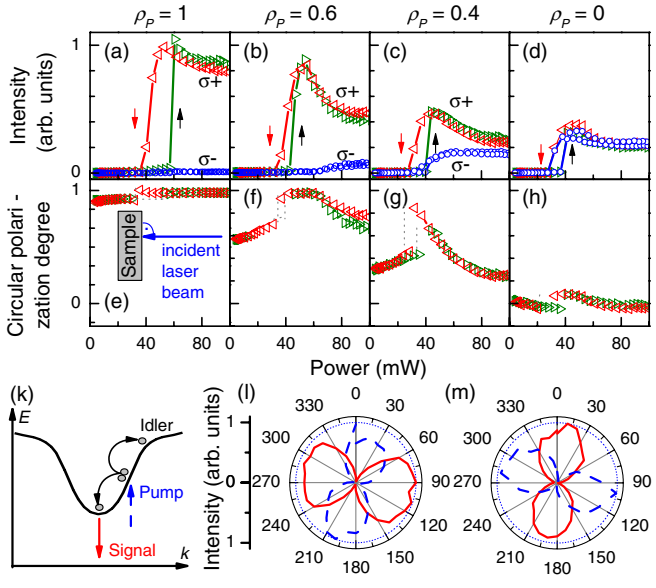


FIG. 1 (color online). (a)–(d) Normal incidence transmitted intensity versus external pump power for $\rho_P = 1$, 0.6, 0.4, and 0. Triangles (blue circles) correspond to the intensity of the $\sigma^+$ ($\sigma^-$) component. Arrows show the direction in which the pump intensity is varied. (e)–(h) Corresponding DCP of transmission versus pump power. Gray dotted lines serve as a guide to the eye. The inset in (e) shows a schematic of the experimental geometry for (a)–(h). (k) Schematic diagram of OPO. (l) and (m) Polar plots of normalized signal (dashed line) and the laser intensity (continuous line) for TE (l) and TM (m) polarized pump.

increasing pump intensity polariton-polariton interactions shift the LP energy towards resonance with the pump energy [9] leading to an abrupt increase of the LP population and hence the transmitted intensity [4,5]. When the pump power is lowered the LP energy jumps back at a lower threshold power, giving rise to a hysteresis loop.

Figures 1(a)–1(d) show the intensities $[I(\sigma^{\pm})]$ of $\sigma^+$ (triangles) and $\sigma^-$ (lines) polarized components of the transmitted beam versus pump power ($I_P$) for various pump DCPs $\rho_P = \frac{I_P(\sigma^+) - I_P(\sigma^-)}{I_P(\sigma^+) + I_P(\sigma^-)}$. The signal is detected from a small region of $2 \times 2$ $\mu$m$^2$, over which the pump intensity is nearly constant. For $\rho_P = 1$, $I(\sigma^+)$ shows an abrupt switch followed by a slow decrease with increasing pump power. A hysteresis loop in the pump power dependence of $I(\sigma^+)$ is observed in accordance with polariton bistable behavior [5]. Notably, on reducing the pump DCP from $\rho_P = 1$ to $\sim 0$ the bistability threshold power and the transmitted intensity at the threshold for the $\sigma^+$-component decrease by a factor of 1.5 and 3, respectively.

The behavior of the minority $\sigma^-$ component versus pump power is different. $I(\sigma^-)$ is zero for $\sigma^+$ circularly polarized excitation (i.e., $\rho_P = 1$), but appears for smaller DCP of the laser until it approaches the same intensity as the $\sigma^+$ component for a nearly linearly polarized pump [Fig. 1(d)]. In the latter case, as expected both $I(\sigma^+)$ and $I(\sigma^-)$ show nearly the same threshold, intensity, and hysteresis loop width. For elliptically polarized pumping at $\rho_P = 0.6$ and 0.4, the $\sigma^-$ component emerges, respectively, at powers 1.5 times larger or nearly equal to the threshold of the $\sigma^+$ component. Surprisingly, $I(\sigma^-)$ exhibits a smooth intensity increase at threshold instead of a steep intensity jump and shows only a weak ($\rho_P = 0.4$) or no ($\rho_P = 0.6$) hysteresis behavior.

The corresponding pump power dependence of the DCP of the transmitted light $\rho_c = \frac{I(\sigma^+) - I(\sigma^-)}{I(\sigma^+) + I(\sigma^-)}$ is shown in Figs. 1(e)–1(h). At very low pump powers in the linear regime the DCP of the pump defines $\rho_c$, which then increases slightly by 10% with increasing pump power. When the threshold power is reached, $\rho_c$ jumps to nearly one for $\rho_P = 0.6$ and 0.4. For $\rho_P = 0$ only a slight change to 0.1 at threshold is observed. With a further increase of pump power, $\rho_c$ decreases again and eventually approaches the pump DCP $\rho_P$ at very high powers. The hysteresis behavior of $\rho_c$ follows that of the $\sigma^+$ component of the transmitted intensity, demonstrating polarization bistability.

The fact that the $I(\sigma^+)$ dependence has 1.5 times lower threshold than $I(\sigma^-)$ at $\rho_P = 0.6$ indicates a difference between the strengths of $\sigma^+\sigma^+$ and $\sigma^+\sigma^-$ polariton-polariton interactions [9]. The sign and the strength of these interactions is strongly influenced by the biexciton resonance [16]. In particular, for pump energies $E_p$ below the biexciton level $2E_p < 2E_X - E_b$ ($E_X$ and $E_b \sim 1$ meV are the exciton energy and the biexciton binding energy, respectively) an attraction (repulsion) between cross (co) circularly polarized polaritons is expected [16].

Attractive coupling between coherent $\sigma^+$ and $\sigma^-$ modes is verified by studying the polarization of the stimulated emission under resonant excitation into the LP branch at $k$ vectors $k_p \sim 1.4$ $\mu$m$^{-1}$. Pump-pump scattering results in formation of a macroscopically occupied signal at $k = 0$ and idler at $k = 2k_p$ in an optical parametric oscillator (OPO) configuration [Fig. 1(k)]. Polar intensity diagrams of the signal (dashed line) and the pump (solid line) are shown in Figs. 1(l) and 1(m) for TE and TM polarized pump, respectively. The orientation of the linearly polarized stimulated emission at $k = 0$ is rotated by $\sim 90°$ with respect to the excitation [17]. The $\sim 90°$ rotation has been observed for pump energies in the broad range 1.5–3 meV below the exciton level. This can only be accounted for by the attractive character of $\sigma^+\sigma^-$ interactions [17].

For weak $\sigma^+\sigma^-$ attractive interactions the bistability threshold of $I(\sigma^+)$ should be at least 4 and 2.3 times less than that for $I(\sigma^-)$ at $\rho_P = 0.6$ and 0.4, respectively [9], according to the ratio of the cross-circularly polarized pump components $I_P(\sigma^+)/I_P(\sigma^-)$. The bistability threshold is expected to be at least a factor of 2 larger for linearly ($\rho_P = 0$) than for circularly ($\rho_P = 1$) polarized pumping. However, we observe in Fig. 1 $I(\sigma^+)$ thresholds at $\rho_P = 0.6$ and $\rho_P = 0.4$ at factors of 1.5 and 1 below $I(\sigma^-)$, respectively, and the ratio of the threshold for $\rho_P = 0$ to $\rho_P = 1$ is $\sim 0.7$. This indicates the strong role of a repulsive blue shift interaction, which shifts the $\sigma^-$ component towards

resonance resulting in a rapid increase of the intensity of $\sigma^-$ when the $\sigma^+$ mode is switched on.

The experimental results can be explained if one takes into account coupling between the coherently driven polariton modes and the incoherent excitonic reservoir, which provides the necessary blue shift. At energies below the exciton emission this reservoir consists of dark exciton states and weakly coupled localized excitons (LE), which introduce additional damping of polaritons [18]. For the inhomogeneously broadened exciton level (FWHM $\sim$ 1.5 meV) in our sample the density of LE states at 2–3 meV below $E_X$ is estimated to be 3–4 orders of magnitude larger than that of polaritons [18].

We adapted the model in Ref. [9] taking into account transitions of the optically driven excitons into the incoherent reservoir in which the overall pseudospin is relaxed. The reservoir provides equal blueshifts for both polarized coherent spin states in addition to the attractive coupling between them which leads to redshift. This is justified since the population is unpolarized due to fast exciton spin relaxation ($\sim$ 20 ps) [19] shorter than the reservoir lifetime ($\sim$ 50 ps) [18]. Our model considers the intracavity $\sigma^\pm$ polarized electric field $\mathcal{E}_\pm$ and coherent exciton polarization $\mathcal{P}_\pm$, respectively, coupled with the exciton population ($\mathcal{N}$) in the incoherent reservoir:

$$i\dot{\mathcal{E}}_\pm = (\omega_c - i\gamma_c)\mathcal{E}_\pm + \alpha\mathcal{F}_\pm + \beta\mathcal{P}_\pm, \tag{1}$$

$$i\dot{\mathcal{P}}_\pm = [\omega_x + V_1|\mathcal{P}_\pm|^2 + V_2|\mathcal{P}_\mp|^2 + (V_1 + V_2)\mathcal{N}/2 - i(\gamma_x + V_r|\mathcal{P}_\mp|^2)]\mathcal{P}_\pm + A\mathcal{E}_\pm, \tag{2}$$

$$\dot{\mathcal{N}} = -\gamma_r\mathcal{N} + 4V_r|\mathcal{P}_+|^2|\mathcal{P}_-|^2. \tag{3}$$

Here, $\mathcal{F}$ is the incident electric field (the pump) taken as a plane wave: $\mathcal{F}_\pm \propto e^{-i\omega_p t}$; $\omega_{c,x}$ and $\gamma_{c,x}$ are eigenfrequencies and decay rates of the intracavity photon and exciton modes; $\alpha$ describes the response of the intracavity electric field to the external pump; $A$ and $\beta$ describe the exciton-photon coupling ($2\sqrt{A\beta}$ is equal to the Rabi splitting); $V_{1,2}$ are matrix elements of the interaction between excitons with the same ($V_1$) and opposite ($V_2$) circular polarizations; $V_1 > 0$, $V_2 < 0$ and $|V_2/V_1| \ll 1$ [17].

The transitions from the coherently driven polariton modes into the reservoir are introduced phenomenologically as exciton nonradiative decay rates in combination with a rate equation for the reservoir occupation [Eq. (3)]. $V_r|\mathcal{P}_\mp|^2$ is the decay rate of the $\mathcal{P}_\pm$ component due to scattering between coherent excitons with opposite $\sigma^\pm$ polarizations. It provides occupation of the reservoir at a rate $4V_r|\mathcal{P}_+|^2|\mathcal{P}_-|^2$ per unit time. $V_r$ may microscopically arise from the scattering of two bright excitons with opposite spin to dark excitons [20]. It may also arise from transitions into the exciton reservoir via virtual creation of biexcitons. Exciton decay into the reservoir due to $\sigma^+\sigma^-$ scattering is likely to dominate over $\sigma^+\sigma^+$ scattering, since in pump-probe experiments in MCs the absorption of a $\sigma^-$ polarized probe is observed to be strongly enhanced by a factor of 3–4 for $\sigma^+$ polarized pumping [18]. $\gamma_r$ is the exciton decay rate in the reservoir. $\gamma_r$ and $V_r$ correspond to effective mean values.

Calculated transmission intensities versus pump power are presented in Fig. 2 for various pump DCP $\rho_P$. The parameters are $V_2 = -0.1V_1$, $V_r = 0.6V_1$, $\hbar\gamma_r = 0.1$ meV, and $\hbar\gamma_x = \hbar\gamma_c = 0.2$ meV which corresponds to the experimental linewidth of polariton emission intensity of $\sim$0.4 meV. The key results of the experiment are well reproduced. First, the decrease in the $\sigma^+$ transmission with increasing pump power [Figs. 2(b)–2(d)] above threshold is observed, which arises from the onset of the nonlinear decay ($V_r$ term) of polaritons as the minor $\sigma^-$ polariton component is populated. This nonlinear decay leads to damping of the $\sigma^-$ component and hence to its smooth increase with pump power without hysteresis at $\rho > 0.6$ [Fig. 2(b) and 2(c)]. Second, the bistability thresholds of both $\sigma^+$ and $\sigma^-$ components are close to each other within 20% at all $\rho_P$ and the maximum intensity of ($\sigma^-$) component decreases with increasing $\rho_P$. Despite the attractive $\sigma^+\sigma^-$ coupling the bistability threshold is 1.5 times higher for circularly than linearly polarized pumping as observed experimentally. This behavior is due to more efficient population of the reservoir by $\sigma^+\sigma^-$ interactions under linearly than circularly polarized pumping, which blueshifts the LP modes and hence reduces the bistability threshold at $\rho = 0$.

If we do not take into account the effect of the reservoir and assume repulsive interaction between cross-polarized polaritons we cannot reproduce simultaneously the observed strong jumps of DCP by 40% with pump power (Fig. 1) and the ratio of bistability thresholds for the cases of circularly and linearly polarized pumps.

Now we show that the polarization bistability leads to the formation of predicted spatial ring patterns of high DCP [10]. Spin rings arise due to variation of the pump power across the excitation region, resulting in polarization bistability thresholds being reached at higher total pump power near the edge of the spot than in the center.

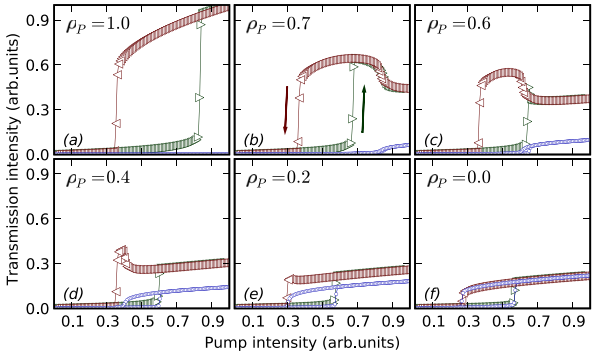


FIG. 2 (color online). The calculated dependences of the MC transmission intensity vs pump intensity, for several DCP of the pump beam ($\rho$). The $\sigma^+$ ($\sigma^-$) component is shown by triangles (blue lines). $\triangleright$ ($\triangleleft$) correspond to increasing (decreasing) pump power. The Rabi splitting, detuning between exciton and photon mode, and detuning between laser energy and LP branch are the same as in the experiment.

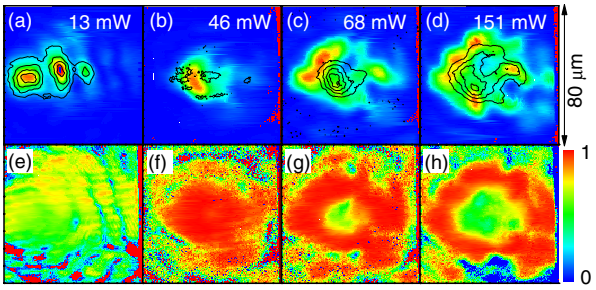


FIG. 3 (color online). Real space images of intensity (a)–(d) and corresponding DCP (e)–(h) of the transmitted beam for elliptically ($\rho_P = 0.6$) polarized pump beam at different pump powers. The images (contour lines) in (a)–(d) show the intensity of the $\sigma^+$ ($\sigma^-$) component.

Figures 3(a)–3(d) show spatial images of the transmitted beam at $\rho_P = 0.6$ for a series of pump powers. Note that below threshold [Fig. 3(a)] both $\sigma^+$ and $\sigma^-$ polarized images are identical and strongly modulated by disorder potential [15]. With increasing power the LP mode in the central area of the spot is blueshifted into resonance with the pump allowing a large intensity of the beam to be transmitted. As the power is increased more the region where the threshold is achieved expands. Note that although the spatial images above threshold [Figs. 3(c) and 3(d)] are still distorted by the disorder they have maxima away from the center of the spot at high power as expected for the case of bistability in a homogeneous sample [15]. This arises since the polariton blueshift above threshold is about ~0.7 meV, which is larger than the amplitude of the disorder potential (± 0.1 meV), hence partially screening polariton energy fluctuations.

Figures 3(e)–3(g) show the corresponding 2D spatial structure of the DCP. Below threshold (13 mW) the DCP is about 0.6, given by the pump DCP. Just above threshold (46 mW) the DCP jumps to unity in the middle of the pump spot forming a disk of high DCP [Fig. 3(f)]. With increasing pump power the DCP in the center of the spot decreases down to 0.5, when the $\sigma^-$ mode switches on [Fig. 1(b)]. At the same time DCP jumps from 0.6 to one in a region forming a ring around the spot center [Fig. 3(g)], where the bistability threshold is achieved for the $\sigma^+$ but not the $\sigma^-$ mode. This ring of high DCP (spin ring) expands with pump power, as the $\sigma^+$ component switches on at larger distances away from the center of the spot [Fig. 3(h)]. Because the potential disorder is partially screened the formation of the DCP rings [Figs. 3(f) and 3(g)] is observed as expected for a pure Gaussian spot [10]. This is consistent with the simulations of Ref. [10], predicting well-defined spin rings even in a disordered system.

In Ref. [10] it was shown that polariton diffusion affects the size of the $\sigma^+$ or $\sigma^-$ polariton modes above threshold and hence the radii of the resultant spin rings, which are determined by the lower bistability threshold. When with increasing pump power the upper threshold is reached at the center of the excitation spot, for example, for the $\sigma^+$ mode, due to polariton diffusion the size of the mode extends to the region with an excitation density corresponding to the lower threshold. By contrast, when with decreasing pump power the lower threshold is achieved in the center of the pump spot, the size of the mode is determined only by that of the Airy mode of the cavity. Experimentally we observe a difference of 30% in the sizes of the $\sigma^+$ modes at the lower and upper bistability thresholds for $\rho_p = 1$ confirming that diffusion affects the spatial distribution of the polariton modes.

In summary, we have observed polarization bistability and spatial spin patterns as a result of spin anisotropy of polariton-polariton interactions. The experimental results are described by effective semiclassical equations of motion taking into account coherent macroscopically occupied modes and an incoherent reservoir.

This work was supported by EPSRC Grants No. EP/G001642, No. EP/E051448, and by RFBR and RAS.

*Note added in proof.*—Recently, experimental results similar to those in Fig. 1 were published [21] although spin patterns and the effect of the reservoir were unexplored. We also note that spin rings have also been reported very recently by another group [22].

*D.Krizhanovskii@sheffield.ac.uk

[1] A. Kavokin *et al.*, *Microcavities* (Oxford University Press, New York, 2007).
[2] P. G. Savvidis *et al.*, Phys. Rev. Lett. **84**, 1547 (2000).
[3] D. N. Krizhanovskii *et al.*, Phys. Rev. B **77**, 115336 (2008), and references therein.
[4] A. Tredicucci *et al.*, Phys. Rev. A **54**, 3493 (1996).
[5] A. Baas *et al.*, Phys. Rev. A **69**, 023809 (2004).
[6] I. Carusotto and C. Ciuti, Phys. Rev. Lett. **93**, 166401 (2004).
[7] A. Amo *et al.*, Nature (London) **457**, 291 (2009).
[8] J. Kasprzak *et al.*, Nature (London) **443**, 409 (2006).
[9] N. A. Gippius *et al.*, Phys. Rev. Lett. **98**, 236401 (2007).
[10] I. A. Shelykh, T. C. H. Liew, and A. V. Kavokin, Phys. Rev. Lett. **100**, 116401 (2008).
[11] A. Amo *et al.*, Nat. Photon. **4**, 361 (2010).
[12] T. C. H. Liew, A. V. Kavokin, and I. A. Shelykh, Phys. Rev. Lett. **101**, 016402 (2008).
[13] M. Kitano, T. Yabuzaki, and T. Ogawa, Phys. Rev. Lett. **46**, 926 (1981).
[14] S. Cecchi *et al.*, Phys. Rev. Lett. **49**, 1928 (1982).
[15] D. Sanvitto *et al.*, Phys. Rev. B **73**, 241308 (2006).
[16] M. Wouters, Phys. Rev. B **76**, 045319 (2007).
[17] D. N. Krizhanovskii *et al.*, Phys. Rev. B **73**, 073303 (2006); P. Renucci *et al.*, Phys. Rev. B **72**, 075317 (2005).
[18] D. N. Krizhanovskii *et al.*, Solid State Commun. **119**, 435 (2001).
[19] A. Vinattieri *et al.*, Phys. Rev. B **50**, 10 868 (1994).
[20] J. I. Inoue, T. Brandes, and A. Shimizu, Phys. Rev. B **61**, 2863 (2000).
[21] T. K. Paraiso *et al.*, Nature Mater. **9**, 655 (2010).
[22] C. Adrados *et al.*, following Letter, Phys. Rev. Lett. **105**, 216403 (2010).